Available online at www.sciencedirect.com
ScienceDirect
Journal of Photochemistry and Photobiology A: Chemistry 189 (2007) 232–238
Journal of Photochemistry and Photobiology A:Chemistry
www.elsevier.com/locate/jphotochem

Synthesis of nitrogen doped TiO_2 by grinding in gaseous NH_3

In-Cheol Kang *, Qiwu Zhang, Junya Kano, Shu Yin, Tsugio Sato, Fumio Saito

Institute of Multidisciplinary Research for Advanced Materials, Tohoku University, Sendai 980-8577, Japan

Received 20 July 2006; received in revised form 15 December 2006; accepted 6 February 2007
Available online 11 February 2007

Abstract

TiO_2 was ground in gaseous NH_3 by using a planetary mill to synthesize nitrogen doped TiO_2. Grinding induces phase transformation of TiO_2 from anatase to srilankite, srilankite to rutile in air at room temperature, whereas the phase transformation of TiO_2 is delayed by the grinding in gaseous NH_3. And, product ground under NH_3 has higher surface area than that of under air, and the heated product displays higher specific surface area than that of product without heating. Light-absorption edge of the products is shifted toward visible light wavelength with an increase in grinding period of time. The ground samples exhibit less photocatalytic activity evaluated by the decomposition of NO gas. This may be due to the existence of residual NH_3 and NH_4^+ formed on TiO_2 surface, which prevents the contact of NO gas with TiO_2 surface. By removing these compositions by thermal treatment at 200 °C for 60 min in air, the photocatalytic activity is improved.

Keywords: Grinding; Nitrogen doping; Gaseous NH_3; TiO_2 photocatalyst

1. Introduction

For efficient utilization of solar energy on photocatalyst, efforts have been put into narrowing its band gap energy. Among many photocatalytic materials, in particular, TiO_2 has been considered as the most popular one, because of its relatively high reactivity and chemical stability under ultraviolet (UV) light [1–3]. The band gap energy of anatase TiO_2 is about 3.2 eV and its absorption wavelength is about 384 nm. For several decades, researches have been performed to narrow band gap by doping transition metals [4–6] or non-metals [7–11] into TiO_2. In particular, nitrogen doping in TiO_2 done by Asahi et al. [7] has prepared by plasma process, resulting in expansion of adsorption edge to about 500 nm in wavelength. Until now, there have been many reports published on preparation of nitrogen doped TiO_2 by various processes and using various nitrogen sources [9,11–13]. However, few researches using gaseous nitrogen source have been reported. The process using gaseous NH_3 as a nitrogen source has various advantages such as no residual organic material and improvement of specific surface area [12]. In this work, TiO_2 was ground in gaseous NH_3 as a nitrogen source by using a planetary mill to prepare nitrogen doped TiO_2. The products were examined by various analytical techniques such as XRD, FT-IR, UV–vis, XPS, SEM, SSA, and its photocatalytic reactivity was evaluated by decomposition of NO gas flow in continuous system.

2. Experimental

2.1. Preparation for grinding

Anatase titania powder (anatase-TiO_2, purity minimum 98.5%, Wako Pure Chem. Inc., Japan) was used as a starting material. A planetary ball mill (Pulverisette-7, Fritsch, Germany) was used for grinding the starting material: the mill consists of a set of pot made of partial stabilized zirconia (PSZ) having 45 cm^3 in inner space, in which seven zirconia balls of 15 mm in diameter were inserted. Four grams of TiO_2 powder were put into the pot, subsequently the pot was set at a tube system where gaseous NH_3 (Purity 99.999%, Daeyangilsan Industry) can be injected into the pot made of stainless steel, after replacement of air, as follows: the air in the pot was pumped out to reach a vacuum of 0.1 MPa prior to injection of NH_3 gas. The grinding was operated at 700 rpm with various grinding periods of time ranged from 15 to 300 min and NH_3 gas pressure at 0.1 and 0.5 MPa. Heating of the ground samples was performed to remove impurities on the surface of the product at 200 °C for 60 min with heating rate at 200 °C/h.

* Corresponding author. Tel.: +81 22 217 5136; fax: +81 22 217 5136.
E-mail address: kic22@andy.tagen.tohoku.ac.jp (I.-C. Kang).

1010-6030/$ – see front matter © 2007 Elsevier B.V. All rights reserved.
doi:10.1016/j.jphotochem.2007.02.003

2.2. Characterizations

The ground products were analyzed by XRD (RAD-B, Rigaku Co., Ltd., Japan) using Cu Kα radiation as a function of grinding periods of time and grinding ambient, respectively.

The specific surface area (SSA) of products was measured by nitrogen adsorption–desorption isothermal measurements at 77 K (ASAP-2010, Micromeritics, Shimadzu, Japan).

In order to demonstrate chemical composition of products and calculate amount of surface adsorbed hydroxyl group/water, infrared spectra were recorded by an FT-IR spectrometer (FTS-40A, Bio-Rad) with the KBr disk method. In particular, in order to calculate surface-adsorbed hydroxyl group/water, the peak intensity related to hydroxyl group/water, positioned around 3440 cm^{-1}, was analyzed.

The absorption edge of the products under irradiation of light was measured by an UV–vis spectrophotometer (UV-2000, Shmadzu, Japan).

NO gas decomposition activity was measured in order to examine photocatalytic activity of the products by measuring the concentration of NO gas at the outlet of reactor box (373 cm^3) with flowing 1 ppm NO–50 vol.% air mixed gas (200 cm^3/min). The photocatalyst product was put on a hollow place of 20 m × 15 m × 0.5 m on a glass holder plate and set in the center of the reactor. A 450 W high-pressure mercury lamp (the irradiation intensity was set in 1000 μmol/s m^2) was used as the light source, in which the wavelength was controlled by various filters, i.e., Pyrex glass for cutting off the light of wavelength >290 nm, Kenko L41 Super Pro (W) filter >400 nm and Fuji, triacetyl cellulose filter >510 nm [14].

X-ray photoelectron spectroscopy (XPS) (PHI 5600 ESCA system, Ulvac-Phi Inc., Japan) was conducted to have the information on chemical bonding energy of the products.

The morphology of products was achieved by SEM technique (SEM, S4100-L, Hitachi, Japan).

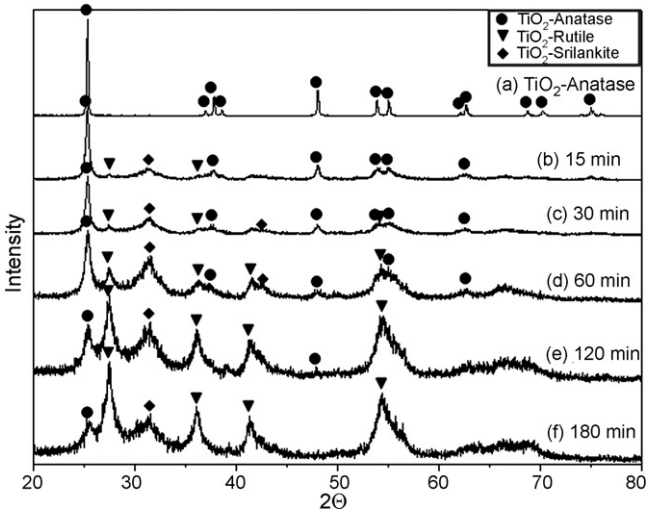

Fig. 1. XRD profiles of TiO_2 ground in gaseous NH3 (0.1 MPa) as a function of grinding periods of time: (a) raw TiO_2, (b) 15 min, (c) 30 min, (d) 60 min, (e) 120 min and (f) 180 min.

3. Results

Fig. 1 shows the XRD patterns of the ground samples. The phase transformation has been observed from the patterns. Srilankite and rutile phases were observed at 15 min grinding, and their intensities continuously increase with an increased in grinding period of time. At 120 min grinding, the srilankite phase diminished in the product, while stable phase of rutile increased.

Fig. 2 verifies that NH_3 gas delays phase transformation of TiO_2 using XRD profiles. Fig. 2A(a–c) represent crystallinity of TiO_2 ground in air, NH_3 (0.1 MPa) and NH_3 (0.5 MPa) by 700 rpm for 120 min without calcinations, and Fig. 2B(a–c) mean phase progressive rate, respectively. The phase progressive

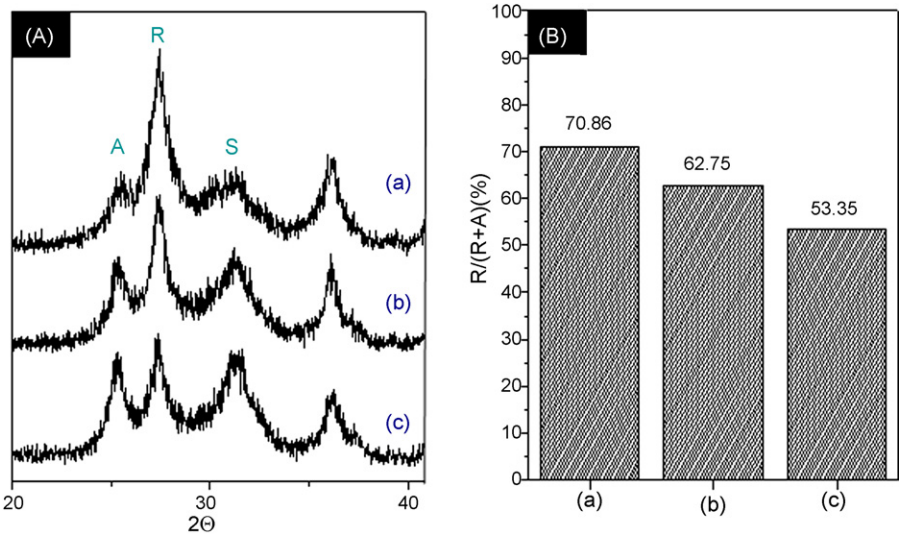

Fig. 2. Comparison of phase transformation progressive rate to rutile ($I_{R(110)}$); (a) ground in air, (b) in NH_3 (0.1 MPa) and (c) in NH_3 (0.5 MPa) for 120 min; (A, anatase; R, rutile; S, srilankite).

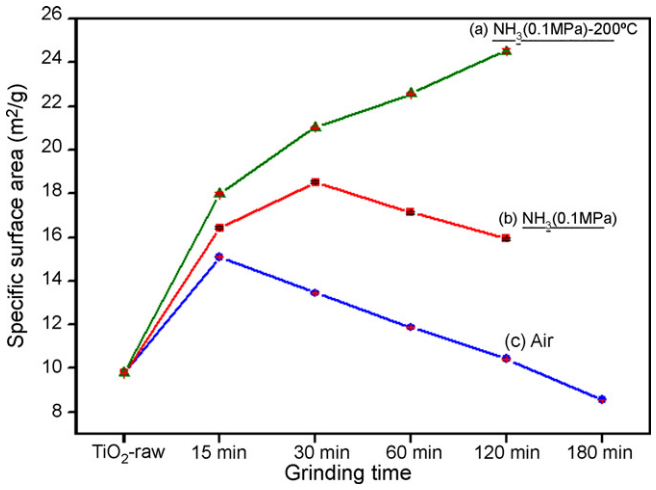

Fig. 3. Comparison of specific surface area depending on the grinding conditions and grinding time: NH_3 (0.1 MPa) with 700 rpm for 120 min heating at 200 °C, (b) NH_3 (0.1 MPa) with 700 rpm for 120 min and (c) Air with 700 rpm for 120 min.

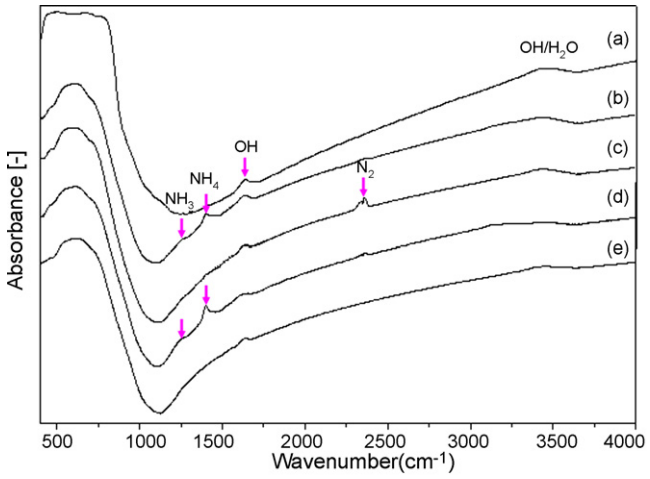

Fig. 4. FT-IR spectra profiles depending on the preparing method: (a) raw TiO_2, (b) ground in NH_3 (0.1 MPa), (c) ground in NH_3 (0.1 MPa) followed by heating at 200 °C, (d) ground in NH_3 (0.5 MPa) and (e) ground in air, respectively.

rates were calculated by following equation:

$$\text{phase transformation progressive rate} = \frac{I_{R(1\,1\,0)}}{I_{R(1\,1\,0)} + I_{A(1\,0\,1)}} \times 100 \quad (1)$$

where $I_{R(1\,1\,0)}$ and $I_{A(1\,0\,1)}$ imply the intensity of rutile (1 1 0) and anatase (1 0 1) phase, respectively. From comparison of phase transformation progressive rate, it is confirmed that the product ground in air appeared the highest phase transformation rate, while the one ground in NH_3 (0.5 MPa) appeared the lowest phase transformation rate. This means that gaseous NH_3 delays the phase transformation of TiO_2 from anatase to rutile phase because of the adsorption of NH_3 on the fresh surface of TiO_2 [12].

Fig. 3 displays SSA value of the sample prepared under various grinding conditions. In the case of product (c) ground in air, SSA continually decreased with grinding time after 15 min grinding, becomes even lower at 180 min grinding than that of the starting sample due to mainly agglomeration. On the other hand, the product (b) ground in NH_3 (0.1 MPa) had higher SSA than that of sample (c) due to non-occurrence of agglomeration for adsorption of NH_3 gas on TiO_2 surface during grinding. But, after 30 min grinding the surface area value decreased continually. This phenomenon is due to an increase in adsorbed NH_3 gas on TiO_2 surface, which may prevent adsorption of liquid nitrogen to sample surface during SSA analysis. Nevertheless, the calcined product (a) after grinding in NH_3 (0.1 MPa), appeared with remarkably improved surface area results throughout grinding period. This result is attributed to removal of surface impurities by calcinations done at 200 °C. From this result, it can be anticipated that grinding of TiO_2 in NH_3 gas and calcination enhance specific surface area.

Fig. 4 illustrates infrared spectra of the products ground in different atmospheres and thermal treatment. Both peaks located at 1635 and 3300–3600 cm^{-1} correspond to hydroxyl group and water molecule [15–18]. Regarding the samples (b) and (d) related to broad peak located at 3300–3600 cm^{-1}, the intensity of sample (d) was weaker than that of (b). This may be due to the reaction of more NH_3 gas with surface hydroxyl group during grinding. On the other hand, peak positioned at 1400 cm^{-1} is clearly observed only with the samples ground with NH_3 gas and the peak intensity of sample (d) was stronger than that of (b). This peak is attributed to NH_4^+ originating from the reaction of NH_3 with hydroxyl group [19,20]. Therefore, the more use of NH_3 results in a stronger NH_4^+ peak in the sample (d).

Looking at the patterns of both samples (b) and (c), the peak at 1400 cm^{-1} has disappeared from sample (c), while it still remained in the sample (b). This indicates that NH_4^+ was removed by heating at 200 °C for 60 min. In the spectra (b)–(d), the intensity of broad peaks seen in the spectra (b) and (d) located at 1249 cm^{-1} related to symmetric mode of NH_3 adsorbed on Lewis acid sites Ti^{4+} [19,21], increased with NH_3 amount. However the peak in the spectrum (c) has disappeared, because of the heating. This is well consistent with the result shown in Fig. 4(c).

The peaks located at 2340 and 2360 cm^{-1} are assigned to adsorption of N_2 on Lewis acid sites and Brønsted acid site, respectively [22,23]. The adsorption of N_2 has been observed in the samples ground in NH_3 gas as well as the heated sample, exhibiting weaker in the ground samples. The peak intensity of products ground in NH_3 was proportional to the injected NH_3 amount. Comparing the spectra (b) and (c), although the 1400 and 1249 cm^{-1} peaks disappear after heating at 200 °C for 60 min, the N_2 adsorption peaks, 2340 and 2360 cm^{-1}, are observed, due to the adsorption of N_2 being in air and originating from decomposition of impurities on the surface of TiO_2 during thermal treatment.

Fig. 5 demonstrates N_{1s} XPS spectra of products ground in (a) NH_3 (0.1 MPa) for 120 min, (b) NH_3 (0.1 MPa) for 120 min followed by heating at 200 °C, (c) NH_3 (0.5 MPa) for 300 min followed by heating at 200 °C and (d) raw TiO_2. All products were measured without sputtering. In spectra of raw TiO_2 (d), weak peak, positioned at 400 eV, was detected, which is assigned to adsorption of N_2 from air. The unheated product (a) dis-

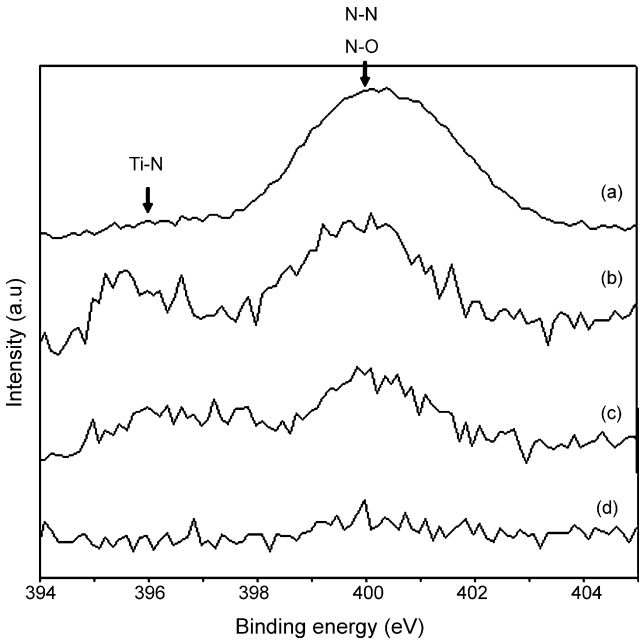

Fig. 5. N_{1s} XPS spectra of products ground in NH_3 (0.1 MPa) for 120 min (a), NH_3 (0.1 MPa) for 120 min heating at 200 °C (b), NH_3 (0.5 MPa) for 300 min heating at 200 °C and (c) raw TiO_2. All products were measured without sputtering.

played strong N–N and N–O bonding energy peaks positioned at 400 eV [7,24], which was stronger than Ti–N bonding peak, located at 396 eV, relatively. This phenomenon verifies the existence of surface impurity such as of NH_3, NH_4^+ and N_2 on the surface of TiO_2 as mentioned in Fig. 4. With the heated samples (b) and (c), both weak peaks positioned around 400 and 396 eV have been observed. This indicates the removal of surface impurities and existence of Ti–N bonding positioned at 396 eV [7]. These results well prove successful nitrogen doping on TiO_2 by grinding in NH_3 gas.

Fig. 6 shows UV–vis spectroscopy patterns of product ground in NH_3 (0.1 MPa) ambient from 15 to 120 min. The absorption

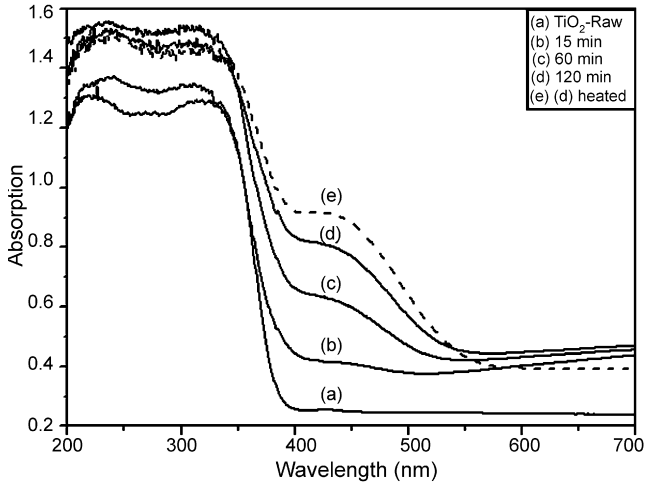

Fig. 6. UV–vis profiles of TiO_2 ground in NH_3 (0.1 MPa) by 700 rpm grinding speed as a function of grinding time: (a) raw TiO_2, (b) 15 min, (c) 60 min, (d) 120 min and (e) (d) heated at 200 °C (Dash).

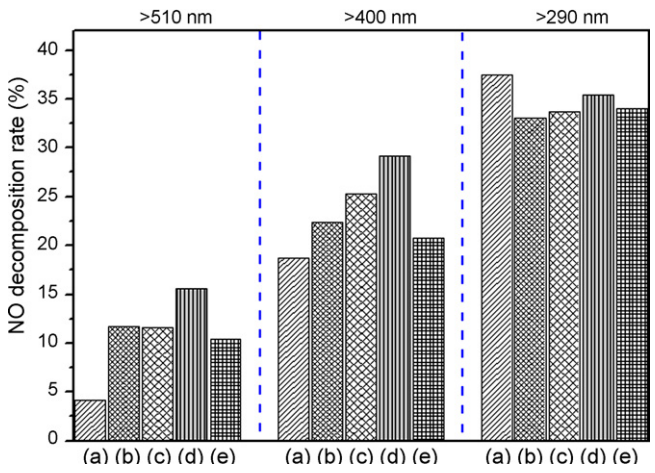

Fig. 7. NO decomposition activity: (a) raw TiO_2, (b) ground for 120 min in NH_3 (0.1 MPa) and heated at 200 °C, (c) ground for 120 min in NH_3 (0.5 MPa) and heated at 200 °C, (d) ground for 300 min in NH_3 (0.5 MPa) and heated at 200 °C and (e) ground for 300 min in NH_3 (0.5 MPa) without heating.

wavelength of raw TiO_2 is below about 384 nm, while that of ground products has been observed to shift toward visible irradiation range and the absorbing area in the visible range increased correspondingly with an increase in grinding periods of time. The results suggest that nitrogen has been doped into TiO_2 and the band gap has been narrowed so that absorbance can occur in the visible range. The doped amount increased with an increase in grinding periods of time. In addition, the patterns (d) and (e) demonstrated that heating improved irradiation adsorption ability due to the removal of surface impurities such as NH_3 and NH_4^+ in present study.

Fig. 7 displays NO gas decomposition activity as a function of grinding periods of time and NH_3 amount. All prepared products demonstrated better NO gas degradation activity than that of raw TiO_2. The patterns in the samples (b) and (c) showed that the NO gas degradation activity in visible light region depends on the used NH_3 amount during grinding. Especially, with regard to the patterns (c) and (d), it was identified that the prolonged grinding enables us to improve photocatalytic characterization, i.e., induction of high nitrogen doping. Consistent with the UV–vis result, the data (d) and (e) verified that heating operation contributes the improvement of the photocatalytic properties of the doped TiO_2 surface for NO gas degradation activity due to the removal of surface impurities such as NH_3 and NH_4^+.

Fig. 8 shows specific surface area (SSA) of the sample under various grinding conditions and post-thermal treatment. As be expected, the SSA values trends closely agreed with NO decomposition activity trends, i.e., NO decomposition activity became high with an increase in SSA value. Unheated product (e) showed lower SSA value compared with heated product (d) for existence of surface impurities.

Fig. 9 demonstrates crystallinity of products by using XRD profiles. Fig. 9A shows XRD patterns, whereas Fig. 9B shows the ratio of rutile phase. In general, anatase phase TiO_2 is the most positive on photocatalytic activity compared with rutile and srilankite. However, Figs. 7–9 results well explained that photocatalytic activity depends on grinding periods and grinding con-

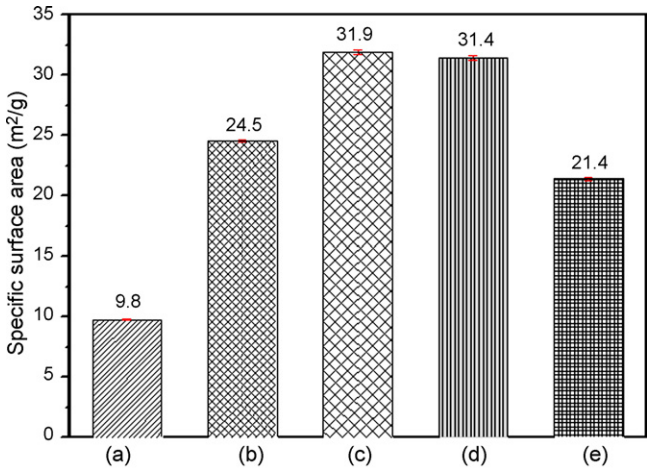

Fig. 8. Comparison of specific surface area with grinding and post-treatment conditions: (a) raw TiO_2, (b) ground for 120 min in NH_3 (0.1 MPa) and heated at 200 °C, (c) ground for 120 min in NH_3 (0.5 MPa) and heated at 200 °C and (c) ground 300 min in NH_3 (0.5 MPa) and heated at 200 °C and ground for 300 min in NH_3 (0.5 MPa) without heating.

dition more than anatase phase ratio. A few papers with regard to relationship between photocatalytic activity and high-pressure phase srilankite have been reported [25], in which anatase TiO_2 has been recognized a better one to photocataltic activity than that of srilakite phase TiO_2. From XRD pattern, the srilankite phase ratio of (b) and (c), respectively, were calculated by following equation; $[(S_{I(1\,1\,1)}/(A_{I(1\,0\,1)} + R_{I(1\,1\,0)} + S_{I(1\,1\,1)})) \times 100]$, in which they have 27.3 and 31.5% srilankite phase ratio, respectively. In Fig. 7, sample (c) showed a better photocatalytic activity than sample (b) in spite of that sample (c) has a higher srilankite phase ratio than that of sample (b). It is understood that it is the doped effect rather than the existing degree of srilankite phase that contributes the improvement of photocatalytic activity.

Fig. 10 illustrates an existing amount of hydroxyl group/water on products surface. These values were obtained by calculating peak intensity connected with hydroxyl group/water peak positioned around 3440 cm^{-1} in FT-IR spectra analysis. The Fig. 10A is a FT-IR profiles and Fig. 10B is peak intensity of 3440 cm^{-1} wavelength. The raw TiO_2 had much

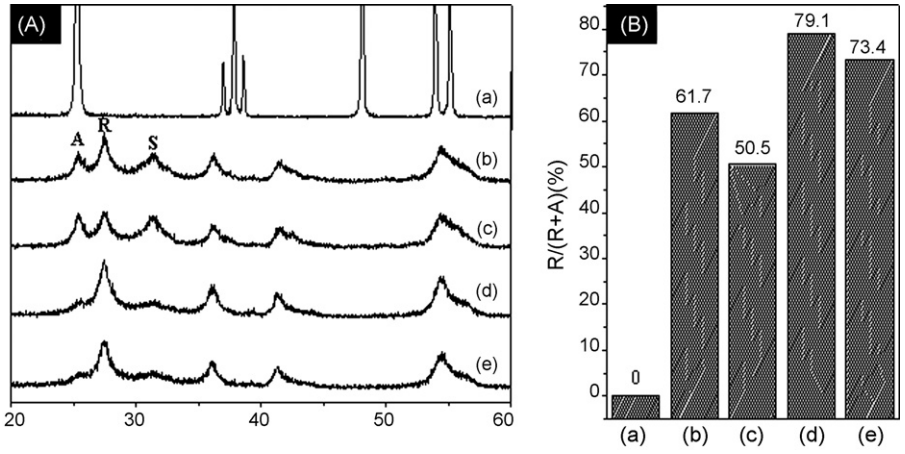

Fig. 9. Crystallinity of products and their rutile phase ratio: (a) raw TiO_2, (b) ground for 120 min in NH_3 (0.1 MPa) and heated at 200 °C, (c) ground for 120 min in NH_3 (0.5 MPa) and heated at 200 °C, (d) ground for 300 min in NH_3 (0.5 MPa) and heated at 200 °C and (e) ground for 300 min in NH_3 (0.5 MPa) without heating.

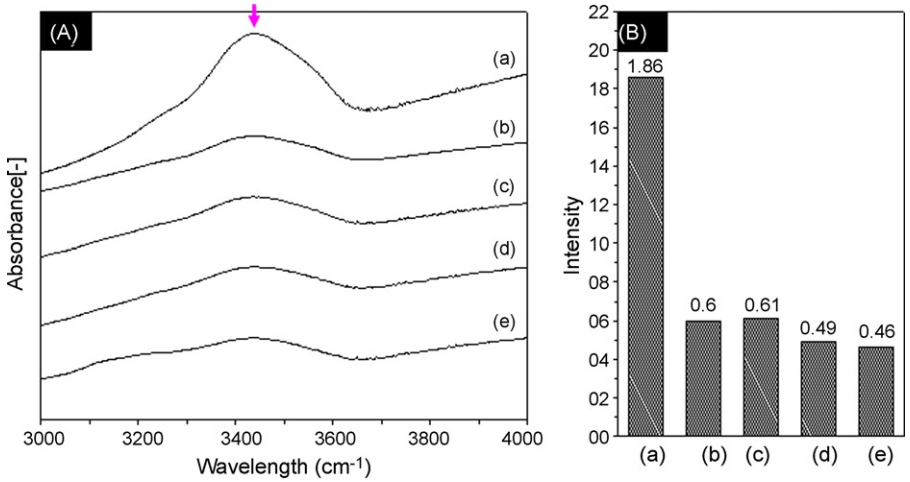

Fig. 10. The intensity of absorbed hydroxyl group and water molecule: (a) raw TiO_2, (b) ground for 120 min in NH_3 (0.1 MPa) and heated at 200 °C, (c) ground for 120 min in NH_3 (0.5 MPa) and heated at 200 °C, (d) ground for 300 min in NH_3 (0.5 MPa) and heated at 200 °C and (e) ground for 300 min in NH_3 (0.5 MPa) without heating.

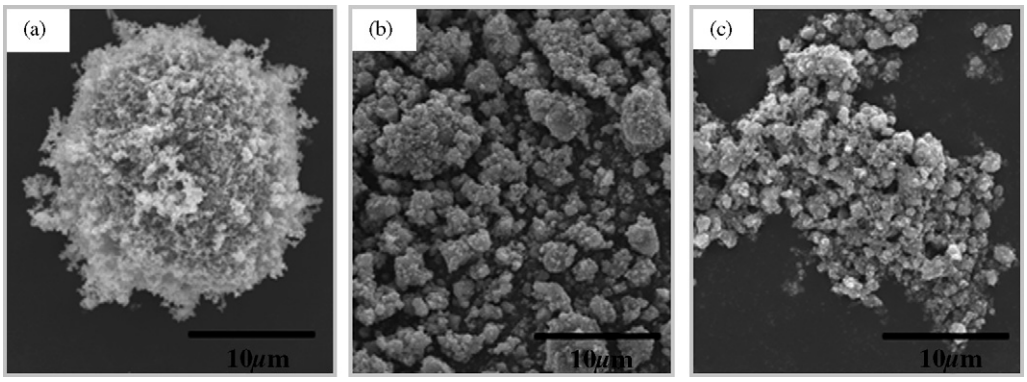

Fig. 11. SEM morphology images: (a) raw TiO_2, (b) ground for 120 min in NH_3 (0.1 MPa) and heated at 200 °C and (c) ground for 120 min in NH_3 (0.5 MPa) and heated at 200 °C, respectively.

hydroxyl group/water, while the ground products contained a little hydroxyl group/water, relatively. The reason may lie in an elimination of hydroxyl group/water by hydroxyl reaction between NH_3 and surface hydroxyl group/water during grinding [26].

Fig. 11 shows SEM morphology of arbitrary region of products: raw TiO_2 (a), product (b) ground in NH_3 (0.1 MPa), and product (c) ground in NH_3 (0.5 MPa), respectively. These SEM results were consistent with photocatalytic activity results (Fig. 7) and specific surface area results (Fig. 8). The spherical raw TiO_2 had 20 μm diameter. The ground and calcined products exhibited finer particles than that of raw TiO_2. In particular, the one ground in 0.5 MPa (NH_3) represented the finest size distribution. By this result, it is confirmed that NH_3 gas is useful to make fine particle as well as N doping during planetary grinding, and particle size decreases with an increase in NH_3 amount.

4. Discussion

This paper discusses the phase transformation of TiO_2 induced by grinding operation at room temperature, followed by the preparation of nitrogen doped TiO_2 induced from the mechanochemical solid–gas reaction. It has been reported that it is easy to induce a phase transformation of TiO_2 with low oxygen pressure during grinding for volume shrinkage by oxygen deficiency [12,27]. Grinding the TiO_2 in NH_3, a retardation of phase transformation has been observed. One possible reason may be due to the adsorption of Lewis base NH_3 at fresh surface of TiO_2. The Lewis base NH_3 and H_2O are easy to adsorb on Lewis acid Ti^{4+}. Since NH_3 gas is more basic than water, if H_2O molecule occupies the most active acidic site before ammonia, ammonia occupies the other unoccupied site or bonds with the hydroxyl groups [26]. Normally, there are two possible pathways for the reaction between NH_3 and H_2O. It is understood, from the changes in enthalpy of two reactions, that the formation of NH_4^+, as given by Eq. (2), are relatively favorable compared with the alternative reaction, as given by Eq. (3) [28]. Therefore, NH_4^+ is formed by hydroxylation between NH_3 and H_2O [19,20], of which the vibration mode is observed in FT-IR spectra [19,21].

$$NH_3 + H_2O \rightarrow H_3N\cdots H{-}OH, \quad \Delta H = -8.15\,\text{kcal/mol} \tag{2}$$

$$NH_3 + H_2O \rightarrow H_2N{-}H\cdots OH_2, \quad \Delta H = -3.46\,\text{kcal/mol} \tag{3}$$

In the NO gas decomposition under irradiation of light ranged from ultraviolet to visible light wavelength, since TiO_2 surfaces are covered by impurities such as NH_3 and NH_4^+ adsorbed, it is not easy for NO gas to contact TiO_2 surfaces due to the covering by such impurities. This is the reason why the ground sample does not demonstrate high photocatalytic activity to decompose NO gas. In addition, the reason that the heated product has higher specific surface area than that of non-heated product (Fig. 3) is also due to existence of surface impurities. Fortunately, these impurities can be desorbed easily by heating at low temperature as 200 °C; this result is confirmed by Fig. 3 (SSA) and Fig. 4 (FT-IR) profiles. In Fig. 7, accordingly, the grinding of TiO_2 in NH_3 gas and heating enhanced NO decomposition activity and specific surface area.

In general, gas compositions such as N_2 and NH_3 have been used to prove the existence of Lewis acid site and Brønsted acid site through adsorption of gases on surface. The FT-IR peaks located at 2340 and 2360 cm^{-1} assigned to the adsorption of N_2 on Lewis acid sites and Brønsted acid site, respectively [22,23] have been observed in the FT-IR spectra of the samples ground in NH_3 gas as well as the heated sample. Such adsorption does not occur in the product ground in air only, therefore it is understood that the nitrogen derived from the decomposition of impurities reacts with TiO_2 surfaces and being in air by grinding and heating. It is interesting to note that the N_2 existence on the TiO_2 surface does not seem harmful to the photocatalytic activity of the prepared sample as observed with the case of NH_3 or NH_4^+.

Comparing the grinding in NH_3 with that in air, the phase transformation of TiO_2 from anatase to rutile TiO_2 during grinding in NH_3 gas has been delayed to certain degree. Since prolonged grinding leads to nitrogen doping, NO gas decomposition behavior on the prepared nitrogen doped TiO_2 has been

improved with an increase in gaseous NH_3 amount as well as grinding periods of time. However, comparing the preparing time of the N-doped sample by using solid nitrogen source such as urea [13], longer grinding time is needed for the nitrogen doping to TiO_2 by grinding in NH_3 gas.

The adsorption of NH_3 and NH_4^+ on TiO_2 surface influences not only the retardation of phase transformation of TiO_2 but the improvement of specific surface area also. The retardation of phase transformation is due to the low oxygen deficiency by covering of TiO_2 surface with NH_3 or NH_4^+ [12].

In Fig. 3, the enhancement of specific surface area of product prepared in NH_3 gas might be due to the prevention of agglomeration between particles for covering of TiO_2 surface by NH_3 and NH_4^+. In comparison (a) and (b), even though (a) and (b) were prepared by same condition i.e., grinding time, rotation speed and atmosphere pressure, the specific surface area values were different for heating process. This implies that the adsorbed NH_3 and NH_4^+ on TiO_2 surface plays as a block for the contact of liquid nitrogen molecules to sample surface during SSA analysis. Similar tendency in UV–vis result in Fig. 6 is observed. Fortunately, the adsorbed NH_3 or NH_4^+ can be easily removed by thermal treatment at 200 °C for 60 min.

In the NO decomposition activity results of Fig. 7, it seems difficult to understand that the raw TiO_2 (band gap energy of 3.2 eV) shows no decomposition ability over 510 nm in wavelength, because the excited electron–hole pair cannot originate under about 387 nm in wavelength [33]. Actually some papers [30–32] have discussed the phenomenon by attributing it to the electron from Ti^{3+}, which locates on below about 0.5–0.8 eV from bottom of conduction band, not the photoexcited electrons from valence band.

For photocatalytic reactions, the adsorbed hydroxyl group/water on surface is important. They react with photoexcited holes on the catalyst surface and make hydroxyl radicals, which is an active oxidant in degrading organics in water [29]. It has been reported that adsorbed water has bands around 3400 cm^{-1} and around 1630 cm^{-1} [18], whereas Ti−OH boding has bands around 3563, 3172 and 1600 cm^{-1} [34]. Moreover, small crystallites could induce the broadness of the peaks [34]. There is a proportional relation between the absorption intensity and the amount of adsorbed species in products. For example, anatase is more active than rutile in adsorbing water and hydroxyl groups [35]. However, in present work, it is difficult to prove an influence of surface-adsorbed hydroxyl group/water on photocatalytic activity. The comparison between (d) and (e) in Fig. 10 well demonstrates the importance of surface purity rather than existence of surface hydroxyl group. In other words, even though sample (d) and (e) include similar hydroxyl group/water, (e) shows less its photocatalytic activity than that of (d) for existing surface impurities such as NH_3 and NH_4^+.

5. Conclusion

The grinding of TiO_2 in gaseous NH_3, followed by heating at low temperature as 200 °C is useful to prepare nitrogen doped TiO_2 for photocatalytic activity under visible-light irradiation. The doping behaviors can be regulated by adjusting NH_3 amount and grinding periods of time and its rotational speed as well. NH_3 atmosphere helped to improve surface area due to the delay of aggregation, and post-heating treatment enhanced photocatalytic activity through improving of surface area by removal of surface impurities such as NH_3 and NH_4^+ related compositions.

Acknowledgement

This work was supported by the Korea Science and Engineering Foundation Grant funded by the Korea government (MOST) (No. 2005-215-D00146)

References

[1] K.I. Hadjiivanov, D.K. Klissurski, Chem. Soc. Rev. 25 (1996) 61–69.
[2] A. Heller, Acc. Chem. Res. 28 (1995) 503–508.
[3] A. Linsebigler, G. Lu, J.T. Yates, Chem. Rev. 95 (1995) 735–758.
[4] A.K. Ghosh, H.P. Maruska, J. Electrochem. Soc. 124 (1977) 1516–1522.
[5] W. Choi, A. Termin, M.R. Hoffmann, J. Phys. Chem. 98 (1994) 13669–13679.
[6] M. Anpo, Catal. Surv. Jpn. 1 (1997) 169–179.
[7] R. Asahi, T. Morikawa, T. Ohwaki, K. Aoki, Y. Taga, Science 293 (2001) 269–271.
[8] W. Ho, J.C. Yu, S.C. Lee, J. Solid State Chem. 179 (2006) 1160–1165.
[9] T. Umebayashi, T. Yamaki, H. Itoh, K. Asai, Appl. Phys. Lett. 81 (3) (2002) 454–456.
[10] S.U.M. Khan, M. AL-shahry, W.B. Ingler Jr., Science 297 (2002) 2243–2245.
[11] S. Yin, K. Ihara, Y. Aita, M. Komatsu, T. Sato, J. Photochem. Photobiol. A Chem. 179 (2006) 105–114.
[12] G. Liu, F. Li, Z. Chen, G. Qing Lu, H.M. Cheng, J. Solid State Chem. 179 (2006) 331–335.
[13] S. Yin, H. Yamaki, Q. Zhang, M. Komatsu, J. Wang, Q. Tang, F. Saito, T. Sato, Solid State Ionics 172 (2004) 205–209.
[14] S. Yin, H. Hasegawa, D. Maeda, M. Ishitsuka, T. Sato, J. Photochem. Photobiol. A Chem. 163 (2004) 1–8.
[15] M. Primet, P. Pichat, M.V. Mathieu, J. Phys. Chem. 75 (1971) 1221–1226.
[16] C. Morterra, J. Chem. Soc. Faraday Trans. 84 (1988) 1617–1637.
[17] S. Musić, M. Gotić, M. Ivanda, S. Popović, A. Turković, R. Trojko, A. Sekulić, K. Furić, Mater. Sci. Eng. B47 (1997) 33–40.
[18] K. Tanaka, J.M. White, J. Phys. Chem. 86 (1982) 4708–4714.
[19] R.M. Pittman, Alexis T. Bell, Catal. Let. 24 (1994) 1–13.
[20] M. Hermann, H.P. Boehm, Z. Anorg. Allg. Chem. 368 (1969) 73–86.
[21] G. Ramis, L. Yi, G. Busca, Catal. Today 28 (1996) 373–380.
[22] J.N. Kondo, S. Shibata, Y. Ebina, K. Domen, A. Tanaka, J. Phys. Chem. 99 (1995) 16043–16046.
[23] F. Wakabayashi, J. Kondo, A. Wada, K. Domen, C. Hirose, J. Phys. Chem. 97 (1993) 10761–10768.
[24] N.C. Saha, H.G. Tompkins, J. Appl. Phys. 72 (1992) 3072–3079.
[25] J. Hu, H. Qin, Z. Sui, H. Lu, Mater. Lett. 53 (2002) 421–424.
[26] B. Boddenberg, K. Eltzner, Langmuir 7 (1991) 1498–1505.
[27] X. Pan, X. Ma, J. Solid State Chem. 177 (2004) 4098–4103.
[28] A.A. Voityuk, A. Blisnyuk, Theor. Chim. Acta 72 (1987) 223–228.
[29] H. Tang, K. Prasad, R. Sanjinés, P.E. Schmid, F. Lévy, J. Appl. Phys. 75 (1994) 2042–2047.
[30] K. Komaguchi, H. Nakano, A. Araki, Y. Harima, Chem. Phys. Lett. 428 (2006) 338–342.
[31] S. Leytner, J.T. Hupp, Chem. Phys. Lett. 330 (2000) 231–236.
[32] G.K. Boschloo, A. Goossens, J. Phys. Chem. 100 (1996) 19489.
[33] C.S. Turchi, D.F. Ollis, J. Catal. 122 (1990) 178–192.
[34] E. Sánchez, T. López, R. Gómez, A. Bokhimi, O. Morales, Novaro, J. Solid State Chem. 122 (1996) 309–314.
[35] Z. Ding, G.Q. Lu, P.F. Greenfiled, J. Phys. Chem. B 104 (2000) 4815–4820.